Electrochemical Measurements on Cells, I: Simulation of Potential Distribution with an Embedded Probe

ECS Transactions, 58 (3) 79-91 (2013)
10.1149/05803.0079ecst ©The Electrochemical Society

Electrochemical Measurements on Cells, I: Simulation of Potential Distribution with an Embedded Probe

Lei Zhang, Feng Liu, and Anil V. Virkar*

Department of Materials Science and Engineering, University of Utah, Salt Lake City, UT 84112, USA

*Contributing Author

Phone: (801) 581-5396

Email: anil.virkar@utah.edu

Finite element analysis is used to calculate electrochemical potential distributions of charged species and chemical potential distributions of neutral species in solid electrolytes of electrochemical cells. Potential distributions of charged species follow the Laplace equation; while that of neutral species are related to the potentials of charged species through the local chemical equilibrium. Simulations with different cell geometries and transport parameters show that an embedded probe with electrically insulating coating along the probe surface (with tips uncoated) is required for the measurement of electrochemical potential of electrons within a solid electrolyte. Simulation also shows that by optimizing both electronic and ionic conductivities, cell stability can be improved.

Introduction

Measurement of electric potential in electrochemical devices such as solid oxide fuel cells (SOFCs), solid oxide electrolyzer cells (SOECs), or oxygen separators are often made by placing a reference electrode on the surface. Measurement of electric potential with embedded electrodes (probes) has also been reported (1). In a typical SOFC, the electronic conductivity is typically negligible compared to the ionic conductivity. In many studies, therefore, the electronic conductivity of the electrolyte is altogether neglected. However, the establishment of local thermodynamic equilibrium, an assumption made inherent in all transport theory, requires that the electronic conductivity cannot be set to zero mathematically (2, 3). Thus, to elucidate the role of electronic conduction in a predominantly ionic conductor, it is necessary to incorporate the electronic conductivity, however small it may be. Also, local equilibrium demands that transport of both ions and electrons (holes) be taken into account to describe the local chemical potential of electrically neutral species, such as oxygen. The local chemical

potentials of electrically neutral species determine the thermodynamic stability and thus also the device stability.

The purpose of the present work is to calculate distribution of electron electrochemical potential, oxygen ion electrochemical potential and oxygen molecular chemical potential inside a typical solid electrolyte used in an SOFC or in an SOEC or in an oxygen separator under an applied voltage.

Theory and Simulation Details

Two typical cell geometries are considered in the simulation: one is an anode-supported cell (Figure 1A); the other is an electrolyte-supported cell (Figure 1B). These cells were simulated under a fuel cell mode and an oxygen separation mode (under an applied voltage).

Electrochemical potential distribution for both electrons and oxygen ions obeys Laplace's equation, as shown in equations 1 and 2 respectively, assuming the ionic and the electronic conductivities are position independent. In the present work, interfacial regions are described by a set of transport parameters and interface thicknesses.

$$\nabla\left(\sigma_e \nabla \tilde{\mu}_e\right) = \sigma_e \nabla^2 \tilde{\mu}_e = 0 \qquad [1]$$

$$\nabla\left(\sigma_i \nabla \tilde{\mu}_i\right) = \sigma_i \nabla^2 \tilde{\mu}_i = 0 \qquad [2]$$

Local chemical equilibrium is described by equation 3.

$$\frac{\mu_{O_2}}{4e} - \phi = \frac{\tilde{\mu}_{O^{2-}}}{2e} \qquad [3]$$

In the above equations, σ_e is the electronic conductivity, σ_i is the ionic (oxygen) conductivity, $\tilde{\mu}_e$ is the electrochemical potential of electrons, $\tilde{\mu}_{O^{2-}}$ is the electrochemical potential of oxygen ions, μ_{O_2} is the chemical potential of oxygen and the electric potential, ϕ is the measurable electric potential related to the chemical potential of electrons μ_e and the electrostatic potential Φ through equation 4.

$$\phi = -\frac{\tilde{\mu}_e}{e} = -\frac{\mu_e}{e} + \Phi \qquad [4]$$

Simulations were performed using both two-dimensional and three-dimensional finite element analysis (FEA). In two-dimensional FEA, PLANE77, a 2-D 8-Node Thermal Solid, is used for meshing as shown in Figure 2A; in three-dimensional FEA, SOLID90, a 3-D 20-Node Thermal Solid, is used for meshing as shown in Figure 2B and Figure 2C. FEA is performed by ANSYS. In all simulations the embedded probe is placed in the middle of electrolyte layer. The parameters for each simulation are listed in Table I.

Results and Discussion

Design of an Embedded Probe

An ideal embedded probe should be able to measure local electric potential without disturbing electric and ionic potential distributions inside the cell. Figure 3 shows the results of two-dimensional simulations with an embedded probe (Figure 3A and Figure 3B) and without an embedded probe (Figure 3C and Figure 3D). In Figure 3A, the electric potential measured at the probe end near the electrolyte surface is the same as the value at probe tip inside the cell. However, the large difference between Figure 3A and Figure 3C as well as the difference between Figure 3B and Figure 3D shows that both electronic and oxygen ion electrochemical potentials distributions are disturbed by the embedded probe. Especially in Figure 3B, there's a large ionic potential drop across the probe, which is inconsistent with the physical picture. This abrupt decrease results from the over-simplified model. A disc sample without an embedded probe can be simulated using a two-dimensional model (Figure 2A) due to the axial symmetry. However, when an embedded probe is introduced, axial symmetry no longer exists. A two-dimensional model with a probe represents a sample with embedded metal sheet, which completely blocks off the ionic current, leading to an abrupt ionic potential drop (Figure 3B).

Figure 4 shows the results of a three-dimensional simulation in the case of an embedded metal probe. Figure 4A and Figure 4B show the electric and the ionic potential distributions at the cross section, which passes through the probe; while Figure 4C and Figure 4D show the cross sections which are far away from the probe. The similarity between Figure 4D and Figure 3D indicates that oxygen ion electrochemical potential distribution is not much disturbed by the embedded probe. However, electronic potential distribution is still disturbed by the embedded probe as can be seen by comparing Figure 4C with Figure 3C. This is attributed to the easy electron migration path along the probe. Coating the embedded probe with a thin insulating shell is thus considered necessary.

Figure 5 shows the results of a three-dimensional simulation with an embedded probe having an insulating coating on the surface of the probe except at the ends. Both electron and oxygen ion electrochemical potential distributions now remain undisturbed as can be seen by comparing Figure 5C with Figure 3C and Figure 5D with Figure 3D. Note the electric potential measured at probe end near the electrolyte surface is still the same as the value at the probe tip inside the cell. These features make an embedded probe with an insulating coating (except at the ends) ideal for electric potential measurement.

Oxygen Chemical Potential Distribution

The thermodynamic stability and also the device stability are determined by the local chemical potentials of electrically neutral species. In the case of SOFC, SOEC and oxygen separators, cell stability is determined by the local oxygen chemical potential. As stated in the theory part, oxygen chemical potential is related to the electron and the oxygen ion electrochemical potentials by the local chemical equilibrium.

Figure 6 shows the results of a three-dimensional simulation in the case of an oxygen separator-1. In an oxygen separator cell, oxygen chemical potentials at the cathode and

the anode are nearly identical since the cathode is exposed to air and the anode oxygen pressure is about 1 atm. In the present simulations, we assumed identical oxygen chemical potentials at both electrodes. By setting μ_{O_2} at both electrodes to zero, Figure 6E and Figure 6F show that the μ_{O_2} in the electrolyte reaches a maximum value of about 1.0 V (with chemical potential given in units of volt) near anode (where O^{2-} is oxidized to oxygen gas) interface. Such a high local chemical potential suggests high oxygen partial pressure which may lead to cell instability, such as cracking or electrode delamination. Indeed, electrode delamination as well as electrolyte cracking has been experimentally observed (4). Electric potential drops linearly across the electrolyte (Figure 6B) since the electrolyte has a very low electronic conductivity. However, the oxygen ion electrochemical potential first sharply rises though the thin anode/electrolyte interface layer and then flattens though the rest of the cell due to the low ionic conductivity in the anode/electrolyte interface layer. Thus, the addition of the two potentials using equation 3 leads to a maximum in μ_{O_2} in the electrolyte near the anode/electrolyte interface. This maximum indicates that the sluggish oxygen ion migration across anode/electrolyte interface leads to the accumulation of oxygen.

Figure 7 shows the results of a three-dimensional simulation in the case of oxygen separator-2, which has the same geometry as oxygen separator-1 but with a larger ionic conductivity in the anode interface layer. This larger ionic conductivity ensures that the anode interface is no longer the rate-limiting layer, and thus oxygen accumulation is suppressed. Comparing Figure 7E with Figure 6E, we note that the highest μ_{O_2} reached in oxygen separator-2 is much lower than that in oxygen separator-1, and it is only localized at the electrode edge (at a singularity). Apart from the edge, the highest μ_{O_2} is about ten times smaller in oxygen separator-2 compared to that in oxygen separator-1. This simulation result suggests that optimizing transport properties is essential to ensure cell stability.

Summary

Using finite element analysis, electrochemical potential distributions of charged species and chemical potential distributions of neutral species were calculated. Potential distributions of charged species are governed by the Laplace equation; while that of the neutral species are determined by the local chemical equilibrium. An embedded probe with an electrically insulating shell (with ends uncoated) is shown to be ideal for the measurement of electric potential. Chemical potentials of neutral species determine cell stability, and by optimizing both electronic and ionic transport parameters, cell stability can be improved.

Acknowledgement

This work was supported in part by the US Department of Energy under its Energy Frontiers Research Centers program at the University of Utah as a flow through from the University of South Carolina (HeteroFoam) under Grant Number DE-SC0001061 (work of Lei Zhang), and by the US Department of Energy under Grant Number DE-FG02-06ER46086 (work of Anil Virkar).

References

1. Lim H.T., Virkar A.V., *Journal of Power Sources*, **192**, 267 (2009)
2. Virkar A.V., *Journal of Power Sources*, **147**, 8 (2005)
3. Virkar A.V., *International Journal of Hydrogen Energy*, **37**, 12609 (2012)
4. Laguna-Bercero M.A., Campana R., Larrea A., Kilner J.A., Orera V. M., *Journal of Power Sources*, **196**, 8942 (2011)

Table I: Simulation Parameters

Systems	**Electrolyte**		**Cathode**		**Anode**		$\Delta\mu_{O2}$	$\Delta\phi$	$\Delta\mu_{O2-}$
	σ_e	σ_i	σ_e	σ_i	σ_e	σ_i			
Units	S/cm	S/cm	S/cm	S/cm	S/cm	S/cm	V	V	V
2D no probe	5E-6	5E-4	5E-4	5E-4	2E-2	1E-3	1.1	1.085	0.015
2D bare probe	5E-6	5E-4	5E-4	5E-4	2E-2	1E-3	1.1	1.085	0.015
3D bare probe	5E-4	5E-4	5E-6	5E-4	2E-2	1E-3	1.1	1.074	0.026
3D coated probe	5E-4	5E-4	5E-6	5E-4	2E-2	1E-3	1.1	1.074	0.026
Oxygen Separator1	1E-4	1E-6	1E-4	1E-6	2E-4	2E-4	0	1.1	-1.1
Oxygen Separator2	1E-4	1E-6	1E-4	1E-4	2E-4	2E-4	0	1.1	-1.1

σe and σi are electronic and ionic conductivities in the demonstrated layer.
$\Delta\mu_{O2}$, $\Delta\phi$ and $\Delta\mu_{O2-}$ are the potential differences across the entire cell.

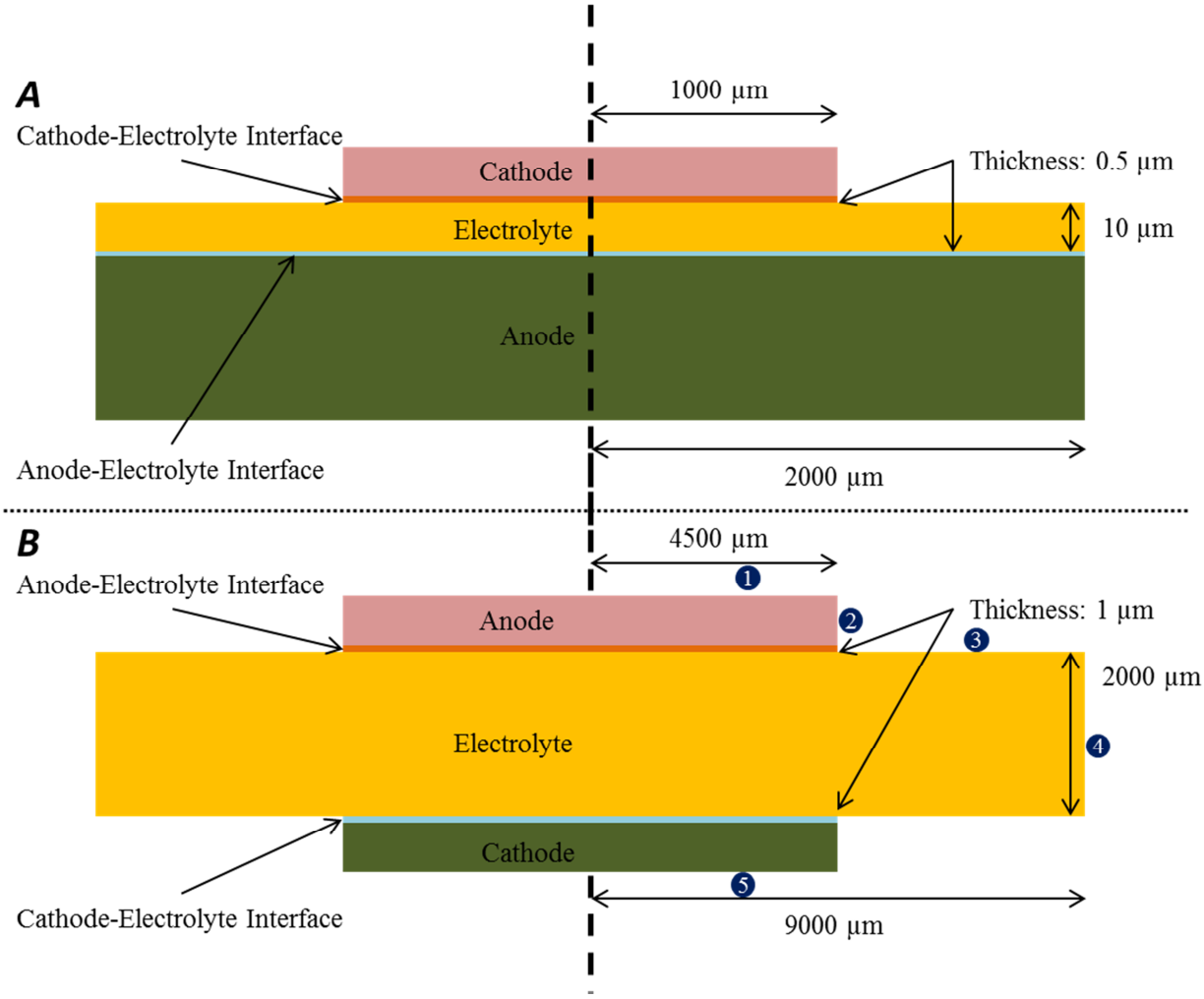

Figure 1: A shows the structure of an anode supported solid oxide fuel cell, and in the simulation it is operated in a fuel cell mode (open circuit condition described here). B shows the structure of an electrolyte supported solid oxide oxygen separation cell. In both cells, the electrodes are equipotential, so their potentials are represented by the potentials at the outer surfaces of the interface layers.

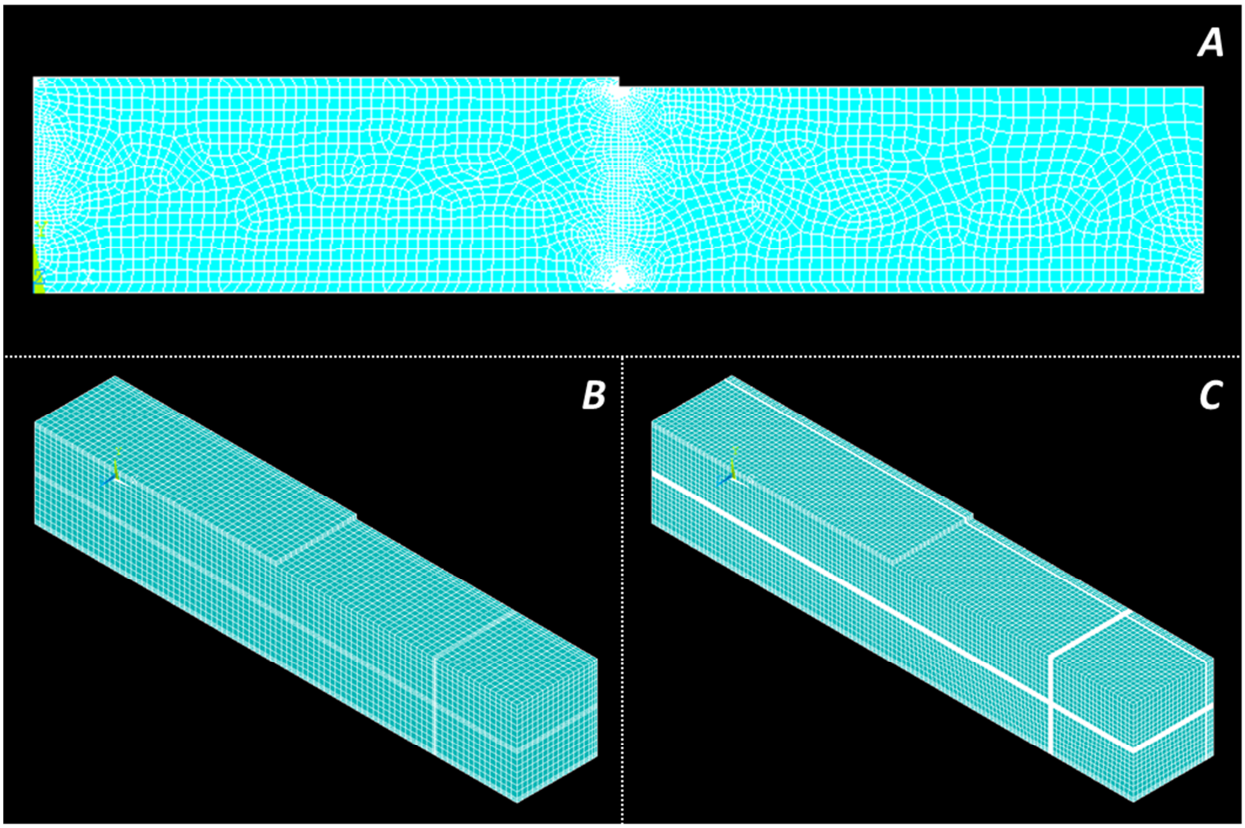

Figure 2: A shows the meshing used in the two-dimensional finite element simulation; B and C show the meshing used in the three-dimensional simulation. All meshing is fine enough such that the calculations rapidly converge.

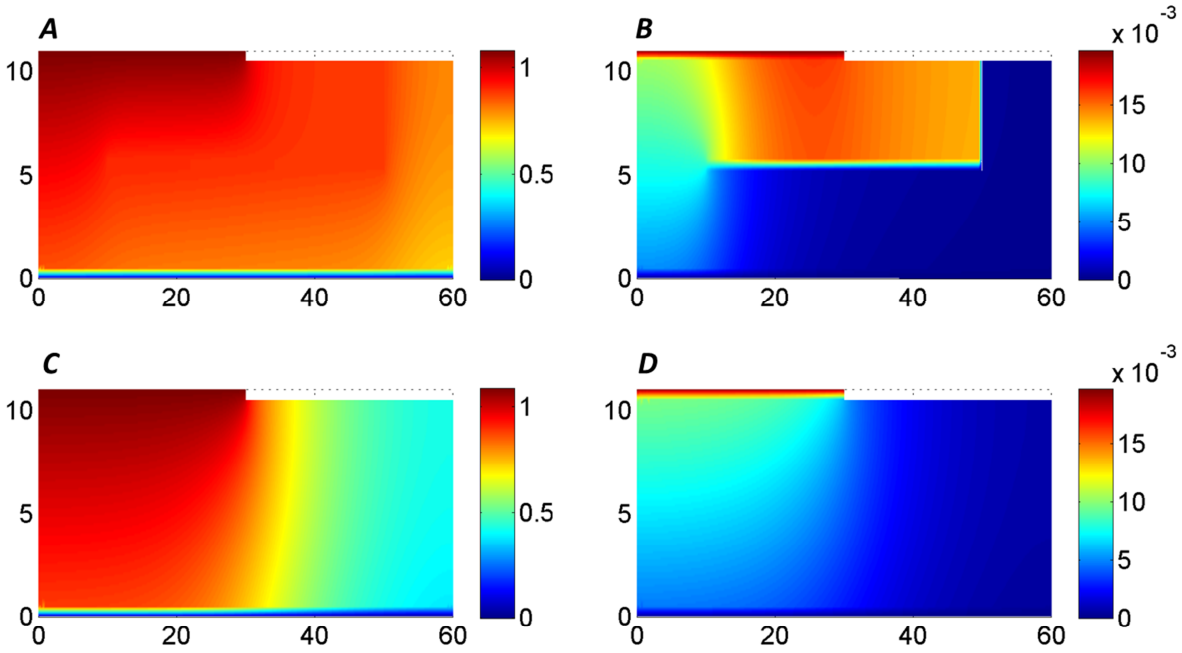

Figure 3: Electric and ionic potentials are plotted in A and B, respectively, for samples with an embedded probe. The potentials plotted in C and D are for samples without an embedded probe, and they are used as a benchmark to determine whether the embedded probe disturbs the potential distributions across the cell.

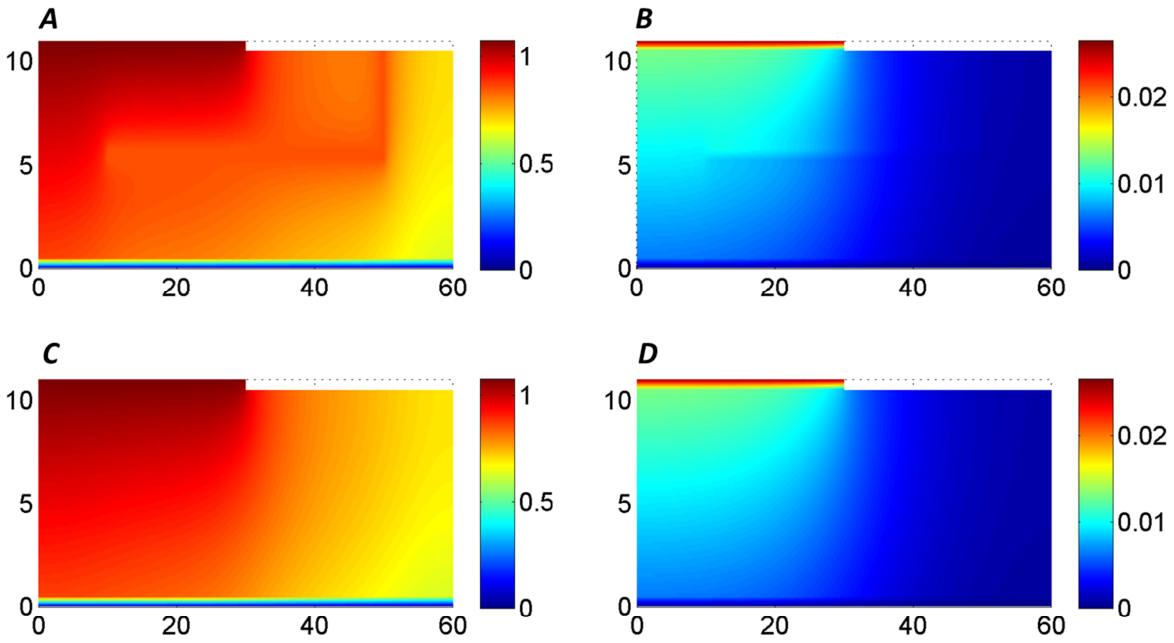

Figure 4: Three-dimensional simulation results, for sample with bare metal probe, are presented in a two-dimensional slide. A and B show electric and ionic potential distributions, respectively, at the cross section though the probe. C and D show the distributions at a cross section far away from the probe, so that they are not disturbed by the embedded probe.

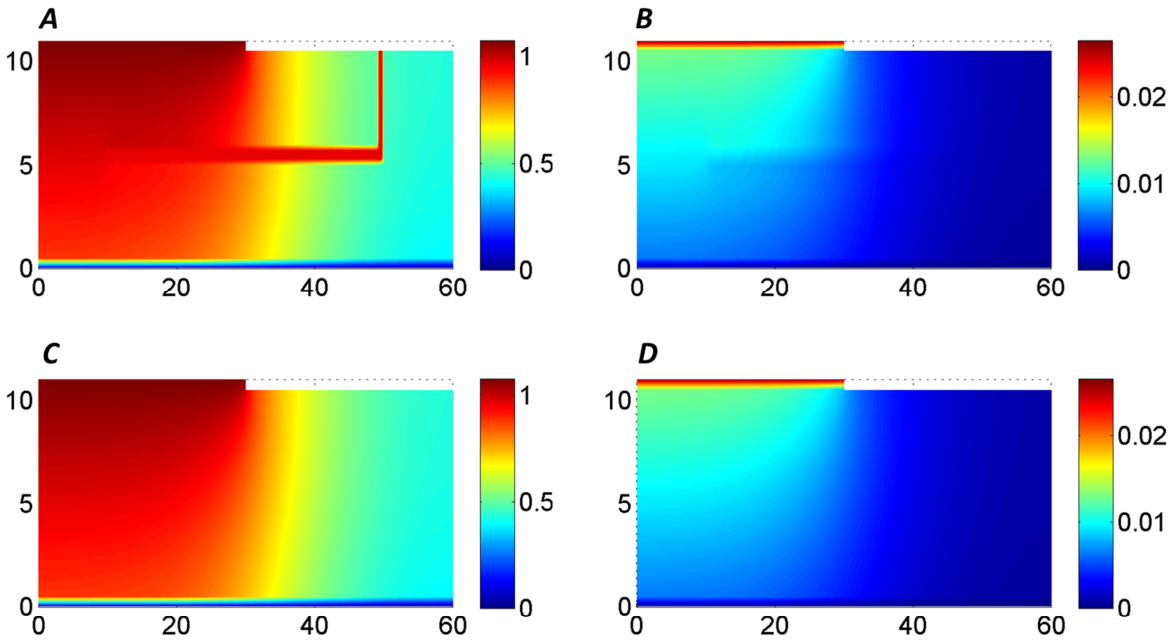

Figure 5: Three-dimensional simulation results for sample with a probe containing an insulating layer along its surface (except at the tips). Note that the presence of the embedded probe with an insulating coating does not significantly disturb the local potentials.

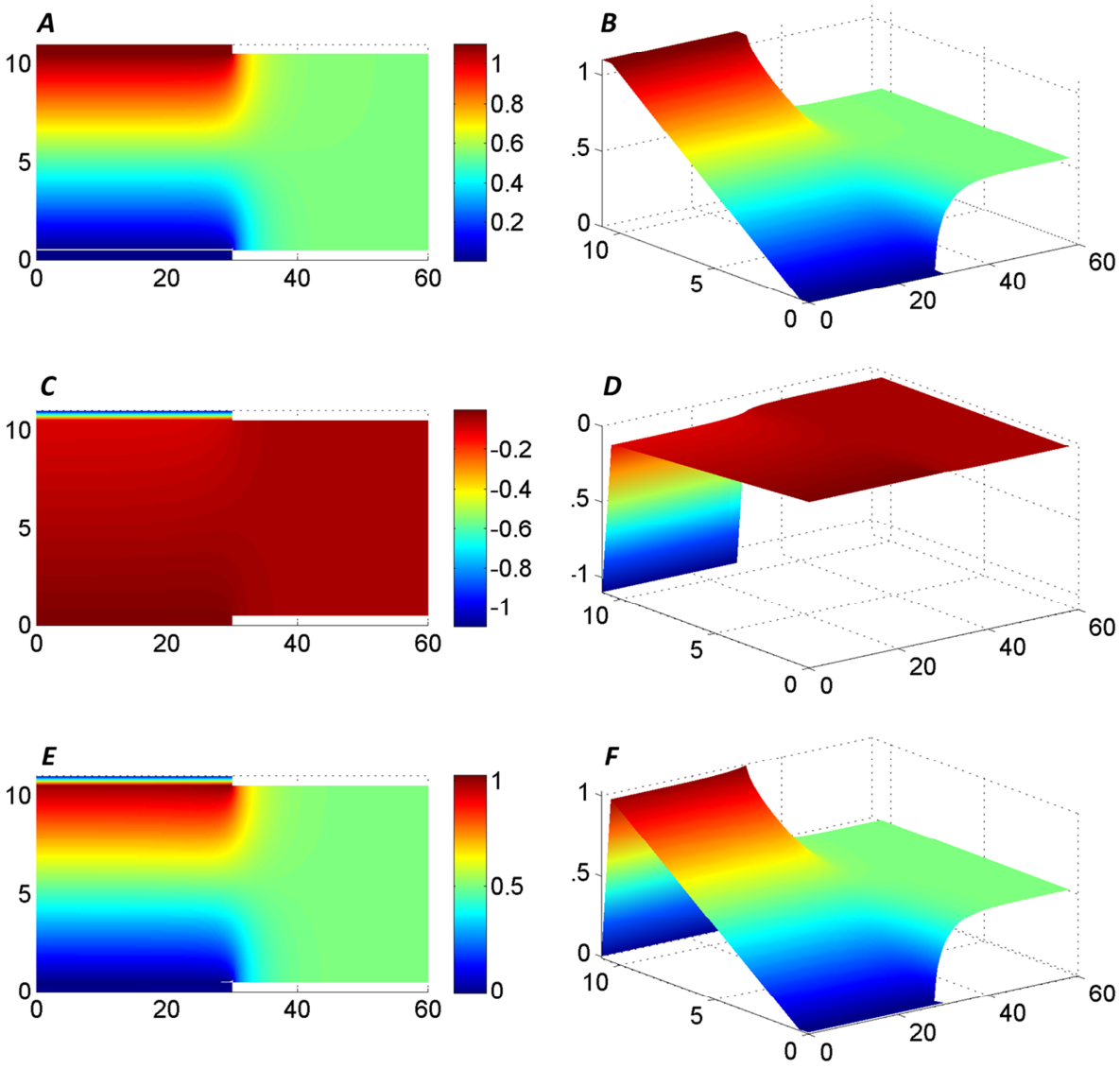

Figure 6: Three-dimensional simulation results for oxygen separator-1. A and B show top and side views, respectively, of the electric potential distributions. C and D show the ionic potential distribution; E and F show the oxygen chemical potential distributions.

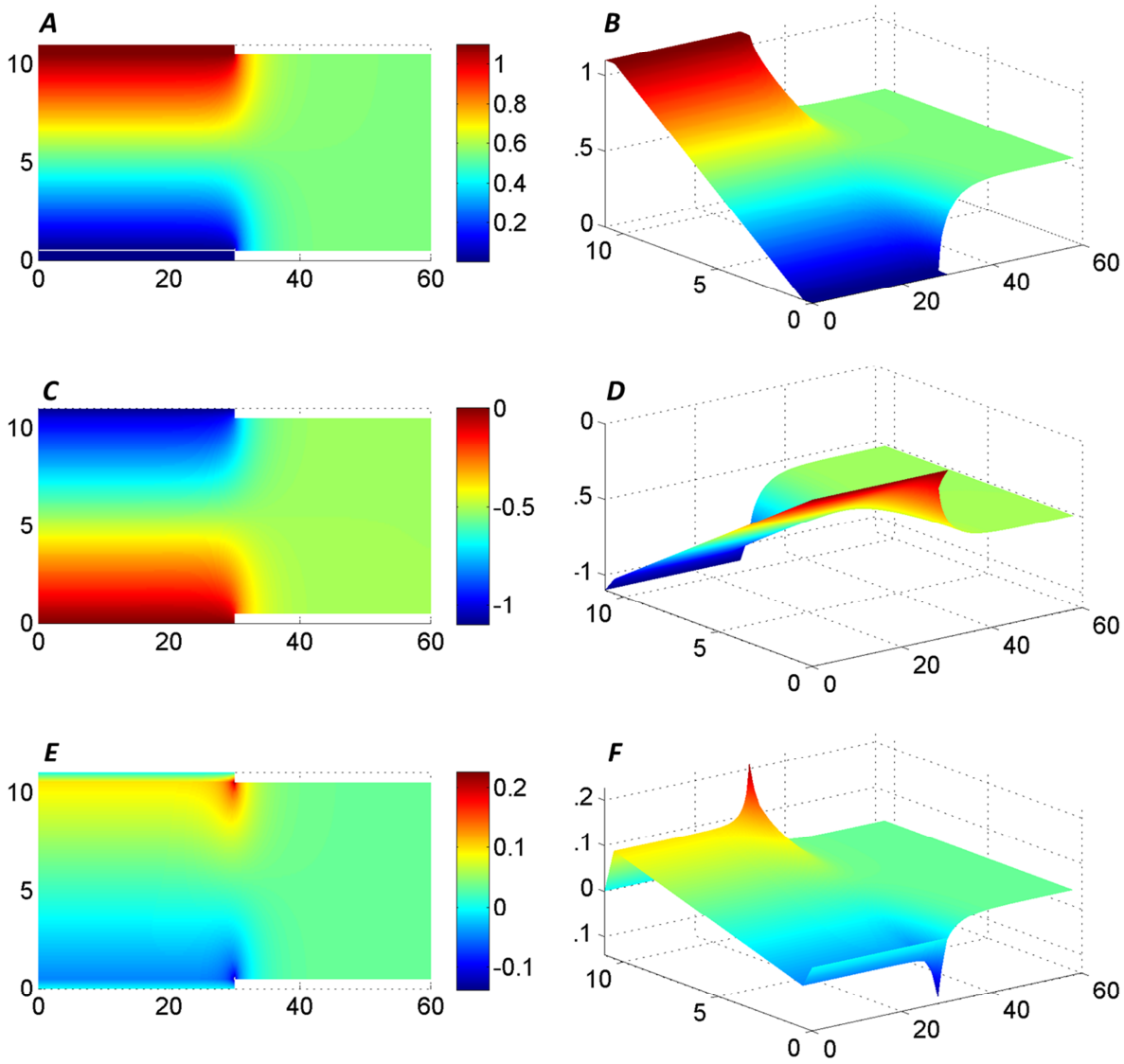

Figure 7: Three-dimensional simulation results for oxygen separator-2.